Resolved Forward Brillouin Scattering in Optical Fibers

R. M. Shelby, M. D. Levenson, and P. W. Bayer
IBM Research Laboratory, San Jose, California 95193
(Received 27 August 1984)

Forward light scattering by the thermally excited acoustic eigenmodes of an optical fiber produces numerous narrow lines not predicted by the bulk-interaction theory of Brillouin scattering. Optical heterodyne detection has been used to resolve the scattering spectrum which begins at about 20 MHz and extends to the detection limit.

PACS numbers: 78.35.+c, 42.80.Mv, 78.20.Hp

A single-mode optical fiber is essentially a long, narrow cylinder of fused silica down the axis of which a single transverse mode of light can propagate, confined by a step in the refractive index.[1] In such a structure, the interaction of light and thermally excited vibrational modes is very different from the bulk scattering described by Brillouin and Mandel'shtam.[2,3] The thermal excitations in a fiber are the eigenmodes of the cylindrical structure rather than the plane waves of the Brillouin theory, and the acousto-optic interaction takes place in a confined geometry that greatly weakens the usual Bragg condition.[4] As a result, the scattered-light spectrum consists of dozens of lines between ~ 20 and 900 MHz. While light scattering in fused silica has long been studied and the vibrational modes of an elastic cylinder constitute a classic problem in mechanics, we are the first to our knowledge to detect and understand the resulting fine structure in the Brillouin spectrum of an optical fiber.[5-7] Our success in detecting the fine structure results from using forward scattering and optical heterodyne detection[8] which gives a better resolution than former techniques.[9,10]

The vibrational modes of a cylinder are characterized by a transverse displacement profile and a wave vector in the direction parallel to the cylinder axis.[5] The transverse profiles can be classified according to the character of their motion as torsional, radial, longitudinal, flexural, or mixtures of these motions. They are assigned azimuthal and radial mode numbers, n and m. The modes responsible for forward scattering light in the core are radial modes independent of ϕ (R_{0m}) or mixed torsional/radial modes varying sinusoidally as 2ϕ (TR_{2m}), the latter being doubly degenerate.[6] The multiplicity of dispersion curves is a key difference between the bulk Brillouin-Mandel'shtam scattering case and the present scattering by guided acoustic waves in an optical fiber. The frequencies detected in our experiment correspond to axial wave vectors near $q_{\parallel}=0$, where all R_{0m} and TR_{2m} modes have nonzero frequency and little dispersion.

Polarized scattering results from the radial dilatation or R_{0m} modes which cause pure phase modulation. To detect this effect, a single-mode fiber must be used as one arm of a Mach-Zehnder interferometer. The other arm of the interferometer transmits the local-oscillator wave necessary for heterodyne detection.[8] The phase fronts, powers, and beam profiles of the two arms are matched on the output beam splitter, and the phase of the local oscillator adjusted to have a component in quadrature with the beam transmitted through the fiber. The interferometer output is detected by a fast silicon p-i-n photodiode, then amplified and dispersed in a radio-frequency spectrum analyzer. The best sensitivity is obtained when the local oscillator nearly cancels the transmitted intensity.[1] It is important that the shot noise of the detection system be at least 3 dB above the thermal noise. We were able to reach that condition with 1 mW of light on the EG&G model FND-100 photodiode and 50 mW of 647-nm light in the optical fiber.

The data reported here were obtained using a 56 cm length of FSV 6000-Å single-mode fiber purchased from Newport Research Corporation. This fiber has a particularly simple internal structure, consisting of a (4.0 ± 0.4)-μm-diam core of germania-doped silica surrounded by a (125 ± 3)-μm-diam cladding of pure synthetic silica.[12] As delivered, the fiber was protected by a jacket of uv-cured acrylate plastic which acted to damp the vibrational modes. When the polymer jacket was removed, the light-scattering spectrum consisted of a rising series of narrow lines the spacings of which approach a constant interval at high frequencies (see Fig. 1).

To detect the TR_{2m} modes, elliptically polarized light is coupled into the fiber core under conditions where the polarization of the output is identical to the input. A Glan-Thompson polarizer after the fiber rejects the linear polarization corresponding to the major axis of the input. The much weaker minor-axis polarization is directed onto the photodiode and acts as a local oscillator in heterodyne detection of the depolarized scattering of light initially polarized along the major axis.[11] Figure 2 shows the more complicated spectrum observed for this polarization. By normalizing the power scattered by the TR_{25} mode in the forward direction to the shot noise power at the base line, we calculated an experimental forward scattering efficiency of $\eta_F=(1.2\pm0.4)\times10^{-12}\ \mathrm{cm}^{-1}$.[11]

We found that the presence or absence of a polymer

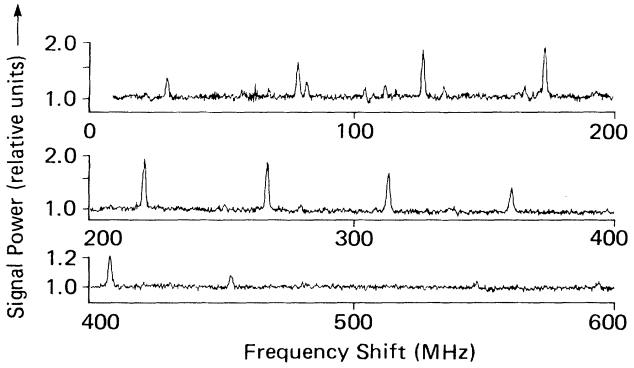

FIG. 1. Polarized guided acoustic-wave Brillouin spectrum. The vertical scale is logarithmic and baseline drift due to the frequency-dependent amplifier response has been subtracted off. The electronic resolution was 1 MHz and the electronic bandwidth of the detection system was 400 MHz. The major peaks correspond to R_{0m} modes and thier frequencies appear in Table I.

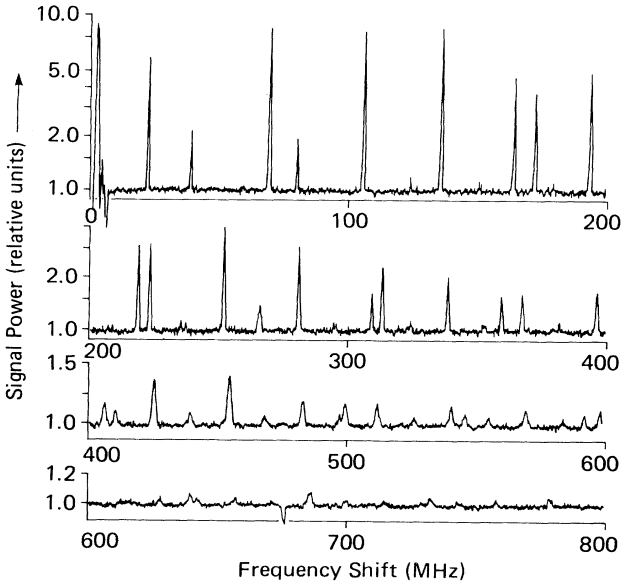

FIG. 2. Depolarized guided acoustic-wave Brillouin spectrum. The electronic resolution was 0.3 MHz below 400 MHz and 1 MHz above. The electronic bandwidth was 1.0 GHz. The base line corresponds to the shot-noise level with 5 mW on the detector. The frequencies of the major components appear in Table I and agree with calculated TR_{2m} mode frequencies.

fiber jacket did not measurably alter the frequencies of the cylinder-guided acoustic waves but did greatly alter the linewidths. The width of the TR_{25} mode at 104.5 MHz was 165 kHz full width at half maximum in the unjacketed fiber and 1000 kHz in an identical jacketed fiber.

The theory of the vibrational modes of a long cylinder has been reviewed by Thurston and by Sittig and Coquin.[5,6] In a uniform cylinder, the frequencies of these modes depend only upon the cylinder radius a, the velocity of longitudinal (dilatation) waves V_d, the velocity of transverse (shear) waves V_s, and the wave vector along the cylinder axis $q_{\parallel}$. The transverse spatial dependence of the modes and their resonant frequencies at $q_{\parallel}=0$ can be determined by solution of the differential equations with the appropriate boundary conditions, in terms of Bessel functions, $J_n(z)$.

For the dilatational R_{0m} modes, the boundary condition corresponding to the free fiber surface can be written as

$$(1-\alpha^2)J_0(y)-\alpha^2 J_2(y)=0, \tag{1}$$

where $\Omega_m = V_d y_m/a$ gives the frequency of the mth mode, $\alpha = V_s/V_d$, and y_m is the mth zero of Eq. (1). For fused silica, $V_2 = 3740$ m/sec and $V_d = 5996$ m/sec.[9] The best fit to experimental spectra was obtained for $\alpha = 0.6203$ and $V_d/2\pi a = 14.801$ MHz, leading to the calculated mode frequencies in Table I.

The displacement of a point within the fiber can be expressed in cylindrical coordinates as

$$U_{rm}(r) = C_{Rm}J_1(y_m r/a), \quad U_{\phi m} = U_{zm} = 0, \tag{2}$$

where C_{Rm} is the amplitude of a thermally excited low-frequency vibration calculated from the equipartition theorem,[7] and is proportional to $(kT)^{1/2}$. For the R_{0m} modes the nonvanishing strain components are

$$S_{rr} = C_{Rm}\left[\frac{1}{r}J_1\left(\frac{y_m r}{a}\right) - \frac{y_m}{a}J_2\left(y_m\frac{r}{a}\right)\right], \tag{3}$$

$$S_{\phi\phi} = C_{Rm}\frac{1}{r}J_1\left(y_m\frac{r}{a}\right). \tag{4}$$

The resulting scalar change in the index of refraction at a point at radius r inside the fiber is

$$\Delta n(r) = \tfrac{1}{2}n^3(P_{11}+P_{12})[S_{rr}(r)+S_{\phi\phi}(r)], \tag{5}$$

where $P_{11}=0.121$ and $P_{12}=0.270$ are the strain-optic coefficients for fused quartz[13] and n is the refractive index. The phase shift, ϵ, of the light propagating down the core can be estimated by averaging of the refractive-index perturbation $\Delta n(r)$ over the mode profile of the guided optical wave. Phase-modulation theory[14] then implies that two sidebands are created, shifted by the vibrational mode frequency $\pm\Omega_m$, and that the forward scattering efficiency for each sideband is $\eta_F = \epsilon^2/4l$ per unit length. The mode radius w is roughly 30 times less than the radius of the fiber a. The Bessel functions in Eqs. (3) and (4) can then be approximated by their lowest nonvanishing term in r for modes which satisfy the condition $y_m/\pi << a/w$. This holds for the first ten or so R_{0m} modes. The

TABLE I. Observed polarized and depolarized scattering frequencies compared to calculated R_{0m} and TR_{2m} frequencies for $a = 64.47\ \mu$m, $V_s/V_d = 0.6203$, and $V_d = 5996.0$ m/s.

Polarized		Depolarized			
Obs. (MHz)	Calc. R_{0m} (MHz)	Obs. (MHz)	Calc. TR_{2m} (MHz)	Obs. (MHz)	Calc. TR_{2m} (MHz)
29.72	29.67	21.52	21.52	405.7	406.5
79.62	79.57	38.20	38.15	410.2	
127.2	126.7	68.41	68.41	425.0	425.0
135.1	TR_{2m}	79.23	78.89	439.3	
173.4	173.5	104.5	104.5		452.5
220.3	220.2		122.8	454.3	454.3
267.3	266.8	135.1	134.9	468.4	
313.6	313.8	163.4	163.2	482.7	482.7
360.4	360.3	171.5	171.4	499.2	499.5
407.2	406.8	192.9	193.8	511.6	511.6
453.6	453.3	218.2	217.8	540.2	540.4
	499.8	222.6	223.3	545.5	546.1
546.6	546.3	251.3	251.6	555.0	
592.7	592.8	265.5	265.2	569.6	569.3
	etc.	280.3	280.6	583.5	
		308.7	309.2	591.9	592.5
		312.8	313.6	598.5	598.2
		338.3	338.4	627.4	627.0
		359.1	359.8	638.9	639.1
		367.2	367.3	614.4	
		396.2	396.1	656.0	655.9
					etc.

shift is then $\epsilon \approx \Delta n(0)\omega l/c$ and the scattering efficiency becomes

$$\eta_F = \frac{n^6\omega^2 kT(P_{11}+P_{12})^2}{32\pi c^2 \rho V_d^2 a^2 B_{Rm}}, \tag{6}$$

where

$$B_{Rm} \equiv [2\pi C_{Rm}^2]^{-1}\int_0^{2\pi}\int_0^1 [U_{rm}^2(y_m x)+U_{\phi m}^2(y_m x)]x\,dx\,d\phi = \int_0^2 J_1^2(y_m x)x\,dx$$

and ρ is the density of the fiber. B_{Rm}^{-1} is proportional to the scattering efficiency per unit elastic energy for a given mode. For the strong polarized R_{03} mode at 127 MHz, these calculations imply a total forward scattering efficiency $\eta_F = 4.4\times10^{-12}$ cm^{-1}, in approximate agreement with the value implied by our observations.

For the TR_{2m} modes, the boundary condition of zero traction at the fiber surface yields a characteristic equation [Eqs. (1) and (2) of Ref. 6] from which the frequencies in Table I are calculated. The calculation of the polarization and phase shift of the light propagating down the core is very similar to, but more complex than, that for the R_{0m} modes. Expressions for U_r and U_ϕ are given in Ref. 6, and all three transverse elements of the strain tensor are nonzero for the TR_{2m} modes. Approximation of the Bessel functions by their small-r expansions is again appropriate for $y_m/\pi << a/w$ and the amplitudes corresponding to thermal excitation can be calculated from the equipartition theorem.[7] The fraction depolarized by the oscillating index perturbations can be calculated[15] by techniques similar to those yielding Eq. (6):

$$\eta_F = \frac{n^6\omega^2 kT(A_1-\alpha^2 A_2)^2(P_{11}-P_{12})^2}{64\pi c^2 \rho V_s^2 a^2 B_{Tm}}. \tag{7}$$

In Eq. (7)

$$A_1 = (6-y_m^2)J_2(\alpha y_m),$$

$$A_2 = (6-y^2/2)J_2(y_m) - 3y_m J_3(y_m),$$

and B_{Tm} is the integral for TR_{2m} modes analogous to B_{Rm}. For the TR_{25} mode at 104.6 MHz, we predict a scattering efficiency of 1.4×10^{-12} cm^{-1} for forward scattering in satisfactory agreement with our measured value of $(1.2\pm0.4)\times10^{-12}$ cm^{-1}. This formalism

also correctly predicts the pattern of relative peak intensities in Fig. 2.

The modes with frequency shifts above rougly 300 MHz do not fulfill our condition $y_m\pi \ll a/w$. When $y_m w/a \approx \pi$, a node will exist within the region sampled by the transmitted light beam giving rise to a partial cancellation of the phase-shifting effect of the vibration. The scattering efficiencies of Eqs. (6) and (7) increase roughly as Ω_m until this cancellation occurs. Beyond that point, the light scattering due to high-frequency modes must drop off with increasing frequency.

In addition to the highly symmetrical FSV fiber, we have studied fibers with elliptical cores and with nonaxisymmetric stress patterns which cause birefringence that can be useful for preserving polarization.[16] Such fibers show similar light-scattering spectra, but some of the degenerate modes are split and polarization selection rules appear. Fibers with different diameters show scattering spectra similar to those presented here with the frequency scale altered by the ratio of the fiber diameters.

In conclusion, we have shown that thermally excited guided acoustic modes cause phase modulation and depolarization of light guided by a single-mode optical fiber. The linewidths of the various frequency components increase with frequency and are dependent on the acoustical characteristics of the material used to sheathe the silica fiber. This light-scattering phenomenon constitutes a thermal noise source within all optical fibers and might ultimately be significant in communications and sensor applications of these devices. While this study has focused on modes with zero wave vector along the fiber axis, corresponding modes exist with nonzero axial wave vector, and these too should be capable of scattering light; in particular, a pattern of splittings similar to that reported here should be detectable in the backscattering case. The potential applications of purposefully excited modes of this type have not escaped our notice.

The authors acknowledge helpful conversations and material assistance from Dr. Roger Stolen and Professor George Stegeman, and the technical assistance of Michael Trump. This research was partially supported by the Office of Naval Research under Contract No. N00014-82-C-0694.

[1]L. B. Jeunhomme, *Single Mode Fiber Optics* (Marcel Dekker, New York, 1983).

[2]L. I. Mandel'shtam, Zh. Russ. Fiz. Khim, Obshchestva **58**, 381 (1926).

[3]L. Brillouin, Ann. Phys. (Paris) **17**, 88 (1922).

[4]J. R. Sandercock, Phys. Rev. Lett. **29**, 1735–1738 (1972), and references therein.

[5]R. N. Thurston, J. Acoust. Soc. Am. **64**, 1–37 (1978).

[6]E. K. Sittig and G. A. Coquin, J. Acoust. Soc. Am. **48**, 1150–1159 (1970).

[7]I. L. Fabelinsky, *Molecular Scattering of Light* (Plenum, New York, 1958). Chap. 7.

[8]D. Marcuse, *Engineering Quantum Electronics* (Harcourt Brace and World, New York, 1971), Chap. 6.

[9]P. T. Thomas, N. L. Rockwell, H. M. van Driel, and G. I. Stegeman, Phys. Rev. B **19**, 4986–4998 (1979).

[10]T. C. Rich and D. A. Pinnow, Appl. Opt. **13**, 1376–1378 (1974).

[11]M. D. Levenson and G. L. Eesley, Appl. Phys. **19**, 1–17 (1979).

[12]Light Wave Technology, Inc., data sheet for type F1506C fiber (1983).

[13]R. W. Dixon, J. Appl. Phys. **38**, 5149 (1967).

[14]A. Yariv, *Quantum Electronics* (Wiley, New York, 1975), Chap. 14.4.

[15]J. C. Kemp, J. Opt. Soc. Am. **59**, 950 (1969).

[16]R. M. Shelby, M. D. Levenson, and P. W. Bayer, Phys. Rev. B (to be published).